Optics Letters

Ultra hybrid plasmonics: strong coupling of plexcitons with plasmon polaritons

SINAN BALCI[1,*] AND COSKUN KOCABAS[2]

[1]Department of Astronautical Engineering, University of Turkish Aeronautical Association, 06790 Ankara, Turkey
[2]Department of Physics, Bilkent University, 06800 Ankara, Turkey
*Corresponding author: sbalci@thk.edu.tr

Received 19 June 2015; accepted 22 June 2015; posted 25 June 2015 (Doc. ID 243135); published 15 July 2015

We report a ternary-coupled plasmonic system consisting of excitons of J-aggregated dye, localized surface plasmon polaritons of Ag nanoparticles, and propagating surface plasmon polaritons of continuous Ag film. J-aggregate dyes are uniformly self-assembled on colloidally synthesized Ag nanoprisms forming plexcitonic nanoparticles, which are placed at a distance nanometers away from the Ag thin film. The reflection measurements, corroborated by theoretical predictions, reveal that the strong coupling of plasmon polaritons and plexcitons results in a newly formed plasmon–exciton–plasmon hybridized state that we call here, reportedly for the first time, a *plexcimon* state. The hybrid plasmonic system shows dispersion characteristics similar to a coupled resonator optical waveguide. The group velocity of the plexcimon state approaches zero at the band edges. The ultrahybrid plasmonic system presented here is promising for a variety of light–matter interaction studies, including polariton lasers, plasmonic devices, plasmonic waveguiding, and spectroscopy.

OCIS codes: (250.5403) Plasmonics; (230.7370) Waveguides; (240.6690) Surface waves.

http://dx.doi.org/10.1364/OL.40.003424

The advancements in top-down and bottom-up nanofabrication techniques as well as the ability to synthesize metallic and semiconducting quantum dots with size- and shape-tunable optical properties have been enabling us to precisely control and deeply understand light–matter interaction at nanoscale dimensions [1–3]. In order to engineer light–matter interactions at nanoscale dimensions, plasmonic systems have recently been combined with excitonic systems. A new hybrid plasmon–exciton mode called plexciton has been observed in the strong coupling regime where the hybrid system shows new optical modes as upper and lower polariton branches. Separation between the branches at zero-detuning is called a Rabi splitting energy [3,4]. A strong coupling regime is appealing because it has direct applications in molecular and material science by changing the optical properties of the emitter or absorber. However, in a weak coupling regime, optical modes are not perturbed, resulting in modification only of emission or absorption of the material (the Purcell effect) [5].

Recently, we have shown colloidally stable plexcitonic nanoparticles demonstrating ultrastrong coupling between the localized surface plasmon polaritons (LSPPs) of Ag nanoprisms (NPs) and excitons of J-aggregates [6]. Herein we show coupling of plexcitons of J-aggregate-coated Ag NPs with the propagating surface plasmon polaritons (PSPPs) of the Ag thin film. The plexcitonic nanoparticles are controllably placed at a distance nanometers away from a silver thin film. Reflection measurements reveal that the strong coupling of plasmon polaritons and plexcitons results in a newly formed hybridized state that we call here for the first time as a plexcimon state. The group velocity of the newly formed optical state is calculated from the dispersion curve. In addition, the new band demonstrates waveguiding behavior similar to a coupled resonator optical waveguide (CROW). The schematic representations of plexciton and plexcimon formations are shown in Fig. 1. In the strong coupling regime, the plexcimon state [hybridized plasmon–exciton–plasmon (PEP)] is observed.

Ag nanoprisms were rapidly synthesized using reaction conditions similar to the previously reported synthesis [6]. In a typical experiment, the seed nanoparticles were synthesized by combining 5 ml trisodium citrate solution (2.5 mM) with 0.25 ml poly(sodium 4-styrenesulfonate) (500 mg/L), and then with freshly prepared 0.3 ml NaBH4 (10 mM). Under the stirring condition, 5 ml $AgNO_3$ (0.5 mM) was added drop by drop at a rate of ~2 ml/min.

Anisotropic Ag nanoparticles were synthesized by varying the amount of seed colloidal solution added to the reaction solution, thereby affecting the morphology or the localized plasmon resonance of the Ag NPs. For example, in a typical experiment, 5 ml of Millipore water was combined with 75 μl ascorbic acid (10 mM) and 60 μl of seed solution to synthesize Ag NPs having an LSPP wavelength of ~750 nm [Fig 2(a)].

Plexcitonic nanoparticles are chemically synthesized by self-assembling a J-aggregate dye on their surface [6]. Recently, similar plexcitonic nanoparticles have been synthesized using another kind of J-aggregate dye [7]. Freshly synthesized Ag

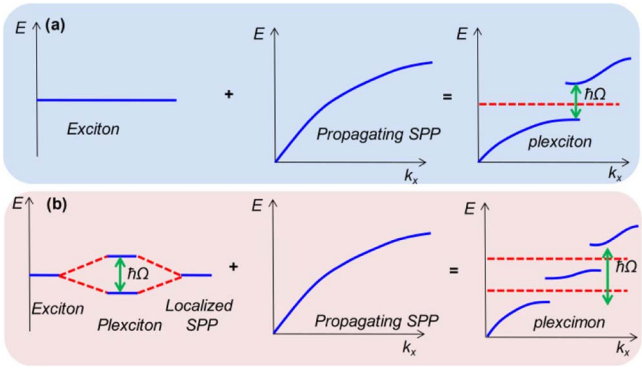

Fig. 1. Schematic representations of (a) plexciton and (b) plexcimon formations in a strong coupling regime.

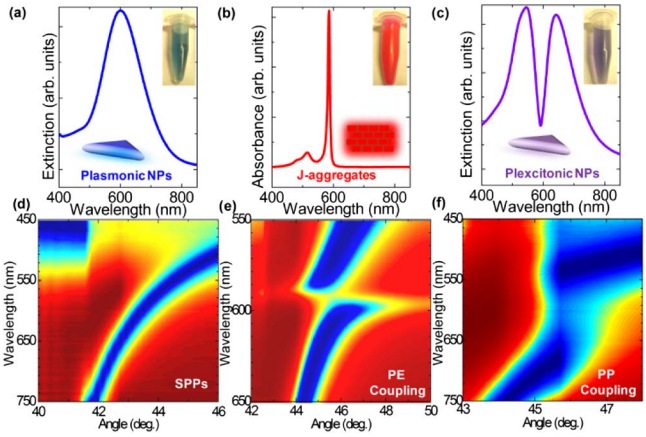

Fig. 2. (a) Extinction spectrum of Ag NPs. The inset indicates the Ag NPs in a reaction vessel, (b) absorption spectrum of J-aggregate, (c) extinction spectrum of plexcitonic nanoparticles. The dispersion curve obtained from (d) bare 10 nm Si_3N_4–40 nm Ag film, (e) Ag film covered with J-aggregates in a PVA matrix, and (f) 10 nm Si_3N_4–40 nm Ag film covered with bare Ag NPs. The blue and red regions indicate the low and high reflectivity, respectively.

NPs are effectively isolated from the reaction by-products by centrifugation. A cyanine dye [5,5′,6,6′-tetrachloro-di-(4-sulfobutyl) benzimidazolocarbocyanine] (TDBC) is purchased from FEW Chemicals. In order to self-assemble TDBC molecules on the nanoprism surfaces, 1 mM TDBC containing 1 mM KBr is prepared [Fig. 2(b)]. The isolated nanoprism solution is combined with the TDBC in KBr solution. Immediately, the color of the nanoprism sol changes [Fig. 2(c)]. Plexcitonic nanoparticles are uniformly and entirely coated on dielectric surfaces by an electrostatic self-assembly process [6]. Prior to the self-assembly process, the dielectric surfaces are modified with 3-aminopropyl-triethoxysilane (APTES) (10 mM in ethanol) and allowed to react for an hour [6]. The APTES modified glass substrates are inserted in the as-prepared Ag NP sol or plexcitonic nanoparticle sol and then the nanoparticles are allowed to electrostatically self-assemble on the functionalized glass surface for 24 h.

Ag thin films were grown on cleaned glass substrates by thermal evaporation of Ag. A dielectric spacer layer of 10 nm Si_3N_4 was deposited by RF magnetron sputtering. The absorption measurements of the bare Ag NPs and plexcitonic nanoparticles were performed using an Agilent Technologies' Cary Series UV–Vis spectrophotometer. Reflection measurements in the Kretschmann configuration (KC) were obtained using a spectroscopic ellipsometer (VASE). The details of the reflection measurements and the coupling of incident light to the surface plasmons have been reported and extensively discussed in our earlier works [8–10]. Figure 2(d) demonstrates the experimentally obtained PSPP dispersion curve of flat Ag film. To study plasmon–exciton coupling on flat 40-nm-thick Ag film, 1.25 mM TDBC in a 0.75% polyvinyl alcohol (PVA) solution was prepared and then spin-coated at 3000 rpm onto the Ag film [Fig. 2(e)]. When the Ag film is covered with a J-aggregate containing ~30-nm-thick PVA film, the coupling of PSPPs of the metal film and excitons of J-aggregates occurs, resulting in formation of plexcitons [8]. In a similar way, when bare Ag NPs are placed at a distance that is nanometers away from the Ag thin film, plasmon–plasmon (PP) coupling is observed [Fig. 2(f)] [10].

After synthesizing plexcitonic nanoparticles, the mixed solution of plexcitonic nanoparticles and dye solution is centrifuged to remove excess dye molecules or J-aggregates not bound to the nanoprisms (Fig. 3). It should be noted here that the J-aggregates also self-assemble on an Ag NP surface without adding KBr. The nanoparticle sol only contains plexcitonic nanoparticles, as shown in Fig. 3.

In both cases (PP and plasmon–exciton), a classical description explains the strong coupling occurring between plasmon polaritons and Lorentzian oscillator that are generating two newly formed optical modes as [3,6–9]

$$\omega_{\pm} = \frac{\kappa}{2} + \frac{\omega_0}{2} \pm \frac{1}{2}\sqrt{A + (\kappa - \omega_0)^2}. \tag{1}$$

When $\kappa = \omega_0$, the Rabi splitting becomes

$$\Omega = \omega_+ - \omega_- = \sqrt{A} = \sqrt{\frac{N}{V}}\frac{e}{\sqrt{\varepsilon_0 m}}, \tag{2}$$

where N/V is concentration of the oscillator, e is electron charge, and m is electron mass. Dispersion of the optical modes are modified under the damping (γ) condition [3,8–10]

$$\omega_{\pm} = \frac{\kappa}{2} + \frac{\omega_0}{2} - \frac{i\gamma}{4} \pm \frac{1}{2}\sqrt{A + \left(\kappa - \omega_0 + \frac{i\gamma}{2}\right)^2}. \tag{3}$$

At resonance condition $\kappa = \omega_0$, the Rabi splitting is

$$\Omega = \omega_+ - \omega_- = \sqrt{A - \frac{\gamma^2}{4}}. \tag{4}$$

As it has been extensively studied in our previous works, it is obvious here that Rabi splitting increases with the square root of the concentration and decreases with an increase in plasmon damping [8–10]. On the other hand, the frequency dependent dielectric constant of metal in a Drude model including damping can be represented as [3]

$$\varepsilon(\omega) = 1 - \frac{\omega_p^2}{\omega^2 + i\gamma\omega}, \tag{5}$$

where γ is the damping rate, and ω_p is the plasma frequency of the metal. The damping term is directly proportional to the

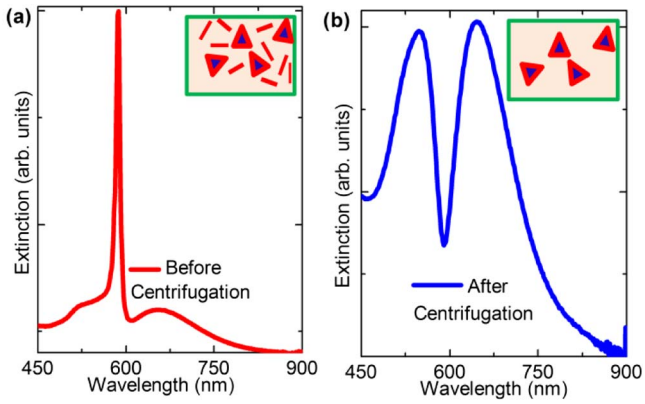

Fig. 3. (a) Extinction spectrum of the plexcitonic nanoparticles and uncoupled (free) TDBC dye molecules before centrifugation. (b) Extinction spectrum of the plexcitonic nanoparticles after centrifugation.

linewidth of the plasmon resonance and inversely proportional to the quality factor of the plasmon resonance [8–10]. In a recently published study, it has also been demonstrated that optical properties of the ultrathin metal films strongly depend on the film thickness [11]. A polariton dispersion curve of 40 nm Ag film covered with 10 nm Si_3N_4 is shown in Fig. 4(a). When the Ag NPs with LSPP resonances at around 600 nm are immobilized onto the dielectric film, a plasmonic bandgap has been formed [Fig. 4(b)] [10]. The lower and upper branches can be described by Eq. (1), and thus the PP coupling is in the strong coupling regime [12–17]. In a similar way, plexcitonic nanoparticles are placed onto the 10 nm Si_3N_4–40-nm-thick Ag film [Fig. 4(c)]. The dispersion curve indicates no new optical modes except the lower and upper plexcitonic modes [3,6,16,17]. Therefore, the PEP coupling is in the weak coupling regime [3]. It is very interesting to note here that plasmonic nanoparticles are in the strong coupling regime [Fig. 4(b)]; however, plexcitonic nanoparticles are in the weak coupling regime [Fig. 4(c)].

In order to observe strong PEP coupling, the thickness of the Ag film has been increased to 60 nm [8]. A reflection curve of 60-nm-thick Ag film coated with 10 nm Si_3N_4 is indicated

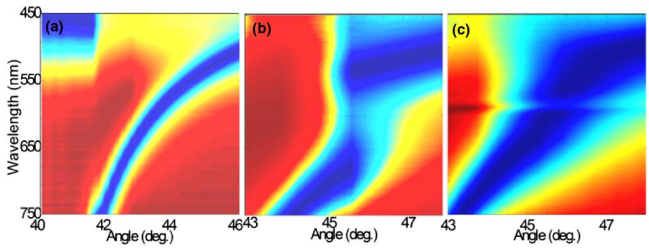

Fig. 4. Strong PP and weak PEP couplings. (a) PSPP reflection curves of 10 nm Si_3N_4–40 nm Ag film. (b) With strong PP coupling, the polariton reflection curve obtained from bare Ag NPs separated from the 40-nm-thick Ag film by a 10 nm Si_3N_4 film. The upper and lower polariton bands are at ~550 nm and ~675 nm, respectively. (c) With weak PEP coupling, the polariton reflection curve obtained from plexcitonic nanoparticles separated from the 40-nm-thick Ag film by 10 nm Si_3N_4.

in Fig. 5(a). The large plasmonic bandgap has been observed when the bare Ag NPs are randomly self-assembled on dielectric-coated 60-nm-thick Ag film [Fig. 5(b)] [10]. The PP coupling is in the ultrastrong coupling regime since the Rabi splitting energy (~700 meV) is very large compared with the plasmon resonance energy of Ag NPs (2.07 eV). In a similar way, plexcitonic nanoparticles are placed onto the dielectric-coated 60-nm-thick Ag films and, subsequently, reflection measurements have been made. The dispersion curve indicates that PEP coupling has now entered into a new regime, i.e., a strong coupling regime because there are newly formed optical modes that we've called plexcimon states (PEP hybrid states) in the dispersion curve [Fig. 5(c)]. The raw data are also shown in Figs. 5(d)–5(f), corresponding to the processed data in Figs. 5(a)–5(c), respectively.

For further analysis of the plexcimon state in the dispersion curve, we have zoomed in on the plexcimon band in Fig. 6(a), which is obtained from the reflectivity map in Fig. 5(c). It should be noted here that when the bare Ag NPs are coated onto the same film structure, large plasmonic bandgap has been observed [Fig. 5(b)]. In the presence of plexcitonic nanoparticles, a new and weakly dispersive localized mode appears inside the bandgap region. The new band suggests that there is a waveguiding mode in the bandgap region.

The waveguiding band can be modeled by using the tight binding approach as also applied to the CROWs [Fig. 6(b)] [18]. Dispersion of the weakly dispersive plexcimonic waveguiding mode by using tight binding approximation can be described as [18,19]

$$\omega(k) = \Omega[1 + \kappa \cos(kD)], \tag{6}$$

where D, Ω, and κ are the distance between the nanoparticles, the resonance frequency of the individual plexcimonic mode, and the coupling coefficient, respectively. D can be altered by

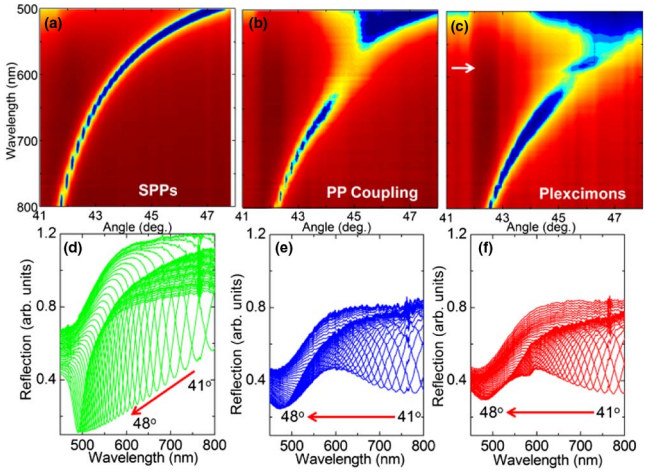

Fig. 5. (a) SPP reflection curves of 10 nm Si_3N_4–60 nm Ag film. (b) Polariton reflection curve obtained from the Ag NPs separated from the 60-nm-thick Ag film by a 10 nm Si_3N_4 film. The upper and lower polariton bands are at ~475 nm and ~700 nm, respectively. (c) Reflection curve obtained from plexcitonic nanoparticles separated from the 60-nm-thick Ag film by a 10 nm Si_3N_4 film. The raw experimentally obtained data are shown in (d), (e), and (f), which correspond to the processed data in (a), (b), and (c), respectively.

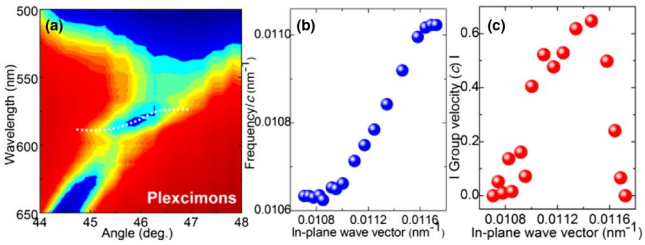

Fig. 6. (a) Dispersion curve (wavelength versus angle) of the plexcimons, (b) dispersion curve (frequency versus momentum) of the plexcimons, (c) calculated group velocity of the plexcimons.

varying the number of plexcitonic nanoparticles on the surface. However, the κ is controlled by a variety of parameters such as dielectric thickness, metal film thickness, and distance between the nanoparticles. Dispersion of the plexcimon mode can be fit by the above equation, and the coupling coefficient between the nanoparticles can be described as $\kappa = \Delta\omega/2\Omega = 0.09$, where $\Delta\omega$ is the bandwidth of the waveguiding plexcimonic band. Therefore, the plexcimonic band observed in Fig. 6(b) can be considered as a weakly coupled plexcimonic state. Furthermore, the group velocity of the plexcimons can be expressed as $v_g = d\omega/dk$:

$$v_g(k) = -\Omega D\kappa \sin(kD). \quad (7)$$

The calculated group velocity from the dispersion curve in Fig. 6(b) shows a sinusoidal profile, as expected from the tight binding approximation [Fig. 6(c)]. At band edges where $k = \pi/D$ or $k = -\pi/D$, the group velocity of the plexcimonic band is very close to zero. The group velocity depends on the coupling coefficient, which is mainly controlled by the dielectric thickness. Another parameter affecting the group velocity is the distance between the nanoparticles, which is controlled by the concentration of nanoparticles on the surface. Indeed, at very low concentrations of plexcitonic nanoparticles, we have observed a flat band of the plexcimonic mode ($v_g \sim 0$) in the dispersion curve. In the case of the thick bottom metal layer (60 nm Ag film), a Fabry–Perot-like cavity forms between the Ag NP and the metal film because the bottom Ag film is sufficiently thick to produce a significant amount of reflection from the bottom layer. Therefore, plexcimons are confined in the cavity region by forming a standing wave. At a high concentration of Ag NPs, the distance between the cavities decreases, and thus individual plexcimonic cavities couple with each other.

It is noteworthy to mention here that with n resonances in the coupled system, $n-1$ transparency dips arise in the dispersion curve as theoretically predicted [20]. In the PEP coupling, for example, three resonances (PSPP, LSPP, and exciton) produce two transparency dips in the dispersion curve.

In summary, we have extensively studied the ternary system of PSPPs of thin metal film, the excitons of J-aggregates, and the LSPPs of metal nanoprisms mutually interacting with each other. In the strong coupling regime, we have observed a new optical state called the plexcimon state, and group velocity of the plexcimons has been calculated. The coupled plexcimons shows CROW-like waveguiding behavior where plasmon loss, dielectric thickness, and plexcitonic nanoparticle density control the dispersion of the plexcimon band. The newly observed plexcimon state is appealing and may find a variety of fundamental and practical applications in understanding light–matter interaction at nanoscale dimension. Therefore, more experimental and theoretical works are urgently needed to fully understand the optical properties of this newly formed optical state and to find interesting applications in areas such as spectroscopy, lasers, and quantum optics.

Funding. Scientific and Technological Research Council of Turkey (TUBITAK) (112T091).

REFERENCES

1. W. L. Barnes, A. Dereux, and T. W. Ebbesen, Nature **424**, 824 (2003).
2. A. F. Koenderink, A. Alu, and A. Polman, Science **348**, 516 (2015).
3. P. Torma and W. L. Barnes, Rep. Prog. Phys. **78**, 013901 (2015).
4. N. T. Fofang, T. H. Park, O. Neumann, N. A. Mirin, P. Nordlander, and N. J. Halas, Nano Lett. **8**, 3481 (2008).
5. E. M. Purcell, Phys. Rev. **69**, 37 (1946).
6. S. Balci, Opt. Lett. **38**, 4498 (2013).
7. B. G. DeLacy, O. D. Miller, C. W. Hsu, Z. Zander, S. Lacey, R. Yagloski, A. W. Fountain, E. Valdes, E. Anquillare, M. Soljacic, S. G. Johnson, and J. D. Joannopoulos, Nano Lett. **15**, 2588 (2015).
8. S. Balci, C. Kocabas, S. Ates, E. Karademir, O. Salihoglu, and A. Aydinli, Phys. Rev. B **86**, 235402 (2012).
9. S. Balci, C. Kocabas, E. Karademir, and A. Aydinli, Opt. Lett. **39**, 4994 (2014).
10. S. Balci, E. Karademir, and C. Kocabas, Opt. Lett. **40**, 3177 (2015)
11. J. Gong, R. Dai, Z. Wang, and Z. Zhang, Sci. Rep. **5**, 9279 (2015).
12. W. R. Holland and D. G. Hall, Phys. Rev. B **27**, 7765 (1983).
13. A. Moreau, C. Ciraci, J. J. Mock, R. T. Hill, Q. Wang, B. J. Wiley, A. Chilkoti, and D. R. Smith, Nature **86**, 492 (2012).
14. J. B. Lassiter, F. McGuire, J. J. Mock, C. Ciraci, R. T. Hill, B. J. Wiley, A. Chilkoti, and D. R. Smith, Nano Lett. **13**, 5866 (2013).
15. E. Prodan, C. Radloff, N. J. Halas, and P. Nordlander, Science **302**, 419 (2003).
16. G. Zengin, M. Wersall, S. Nilsson, T. J. Antosiewicz, M. Kall, and T. Shegai, Phys. Rev. Lett. **114**, 157401 (2015).
17. D. E. Gomez, H. Giessen, and T. J. Davis, J. Phys. Chem. C **118**, 23963 (2014).
18. A. Yariv, Y. Xu, R. K. Lee, and A. Scherer, Opt. Lett. **24**, 711 (1999).
19. A. Kocabas, S. S. Senlik, and A. Aydinli, Phys. Rev. Lett. **102**, 063901 (2009).
20. C. W. Hsu, B. G. DeLacy, S. G. Johnson, J. D. Joannopoulos, and M. Soljacic, Nano Lett. **14**, 2783 (2014).